JOURNAL OF SOLID STATE CHEMISTRY **1**, 376–385 (1970)

The Tensimetric Reflection of Atomic Order

LEROY EYRING

Department of Chemistry, Arizona State University,
Tempe, Arizona 85281

Received October 9, 1969

Phase reactions between the iota phase (M_7O_{12}) and those contiguous to it in the pure praseodymium and terbium oxide systems and in the ternary praseodymium–terbium–oxygen and terbium–cerium–oxygen systems are discussed in detail. Tensimetric studies have revealed reproducible nonclassical behavior described as pseudophase formation in the hysteresis loops of the two-phase regions. Examination of these phase reactions by high-temperature X-ray analysis as they occur has given additional information. The behavior of these systems is described in terms of microdomain formation derived from iota and the contiguous phases coherently intergrown.

A parallel is suggested between these observations and the intergrowth and block structures in oxides which were among the last objects of study of David Wadsley.

Introduction

There was an elegant economy in the intellectual and physical activity of David Wadsley whether reflecting on atomic arrangements of the atoms in inorganic solids or exploring the contours of the southern Australian beaches with his family and his dog. A few well-conceived ideas and motifs guided his life's work like the themes of a Beethoven symphony.

A dominant motif was the idea of consistent atomic coordination and its preservation in atom-deficient materials by crystallographic shear. He sensed a hierarchy of atomic ordering as oxides change their composition yet preserve simple coordination by economizing on oxygen by the occurrence of crystallographic shear in infinite sheets or prisms. He had explicit doubts of the stability of phases of wide composition range having high concentrations of vacancies or interstitials. He viewed these rather as cases of considerable short-range order which should ultimately separate into completely ordered structures or intergrowths of more than one ordered structure.

What are the thermodynamic consequences of these ideas in binary solids in which one of the components is volatile? What happens to the chemical potential of each component in the progressive sequence of order from short to long range? Of course, the thermodynamic behavior of systems at equilibrium are correlated without need of specifying or acknowledging their atomic nature, nevertheless, these properties are concomitant with the structural changes occurring at the atomic level.

At present there are no complex oxide systems for which the structural and thermodynamic properties have all been determined and correlated. This is a rational goal for the future. On the one hand, we have oxide systems such as those brilliantly illuminated by the structural work of Wadsley and his contemporary inorganic crystallographers and on the other oxide systems carefully studied thermodynamically. It is desirable to relate the chemical potential of the components of such systems to their detailed structural behavior.

In the experiments to be described in this paper the equilibrium oxygen pressure is observed as a measure of the oxygen activity in the binary and pseudobinary fluorite related phases of the rare earths. In these refractory materials there is a high mobility of oxygen and a rapid adjustment of the oxygen sublattice, but the metal atoms maintain their essentially fluorite positions. Oxygen equilibrates *very* rapidly with these fine crystalline powders to give products which change at a vanishingly slow rate, if at all, at temperatures above about 400°C and pressures high enough to transport the required oxygen rapidly to the reaction surface. This leads to complete reversibility in the single-phase regions and quite reproducible hysteresis and pseudophase (phases which are bivarient in one reaction direction only) behavior in the two-phased regions. (The ever-present gaseous oxygen phase is implicit in all future discussion.) In fact, there are no infinitely abrupt line phases rather definite ranges of composition which are narrow or quite broad.

The main purpose of his paper is to illustrate the intricate tensimetric behavior which accompanies the subtle but extensive structural changes (most of which are as yet unknown) presaged by the remarkable insights of David Wadsley.

In the sense implied above, each solid specimen is unique. A complete characterization would reveal compositional or spatial distinctions which establish its uniqueness. Such a total characterization is as yet unfeasible, so that we do, as a practical matter, speak of certain specimens as being of the same phase when differences are not discovered by accepted thermodynamic methods. More sophisticated tests for sameness are now possible, however, and differences are discovered where none were apparent before.

Nonstoichiometry

Since at equilibrium solid phases possess their components at the same chemical potential as they exist in the environment, all phases must have a range of composition which depends on the environment including such variables as temperature and pressure.

If the composition of the phase has a very narrow range and its components may be represented as being in the ratio of small whole numbers, it is termed a stoichiometric phase. Such phases are probably less common than usually believed. On the other hand, if variability of composition is appreciable, the phase is said to be nonstoichiometric. This variation may be trivial as in the alkali and alkaline earth metal oxides which are said to be stoichiometric or extensive as in certain transition metal oxides existing in varying partial pressures of oxygen.

Among oxide phases exhibiting gross variability in composition many have been shown to be unstable toward unmixing resulting in two new phases of small variability of composition. The question has been raised, by Wadsley among others, as to whether any grossly nonstoichiometric phase is thermodynamically stable.

Beyond the question of stability or stoichiometry of chemical substances is the character of their defect structure. Of course, at all temperatures above the absolute zero there are defects, the equilibrium concentrations of which depend on the energy and entropy required to form them. In stoichiometric phases at moderate temperatures these are usually considered as random point defects. On the other hand, in grossly nonstoichiometric or defective materials random point defects or small clusters are uneconomical in energy compared to the ordering of these defects into a new structural feature.

There is a substantial current effort to develop a comprehensive understanding of chemical systems exhibiting such extended defects. This effort includes structural, thermodynamic and kinetic studies as well as theoretical considerations in terms of order–disorder theory and the thermodynamics of small systems applied to microdomains (*1*).

Phase Transformations

In addition to carefully mapping out a phase diagram it is of interest to observe the behavior of the phases in transition especially where they occur between phases of narrow and wide composition range. Complete studies must lead ultimately to a knowledge of the mechanism of solid-state reactions. These reactions involve order $\rightleftharpoons$ disorder changes and commonly display chemical hysteresis and pseudophase behavior in the two-phase regions. In this connection the extensive consideration (*2*) of premonitory behavior in melting and hybrid crystal formation by Ubbelohde is certainly relevant.

The Rare-Earth Oxide Systems

The rare-earth oxides afford a particularly favorable set of model systems of solid-state behavior, since they display a progressive polymorphism in their sesquioxides, numerous analogous intermediate stoichiometric oxides, as well as examples of genuinely nonstoichiometric phases.

Specifically, in the praseodymium–oxygen system, a sequence of compounds of narrow composition range may be represented as a homologous series with the formula Pr_nO_{2n-2} (phases with $n = 4, 7, 9$ $10, 11, 12$, and ∞ have been identified) as well as two nonstoichiometric phases which at higher temperatures and pressures cover the entire composition range between $PrO_{1.5}$ and PrO_2 except for a narrow miscibility gap (*3*). Figure 1 gives the compositions and phase relationships in this system. This diagram, supported by much other evidence from previous work, was constructed from expressive isobars similar to those illustrated by the selection in Fig. 2. A glance at these curves makes one conscious of the richness of information concerning phase reactions provided in (p, t, x) studies which is lost in the projection to the phase diagram. In these curves, not only the stable single-phase regions (where the heating and cooling curves coincide) are seen, but

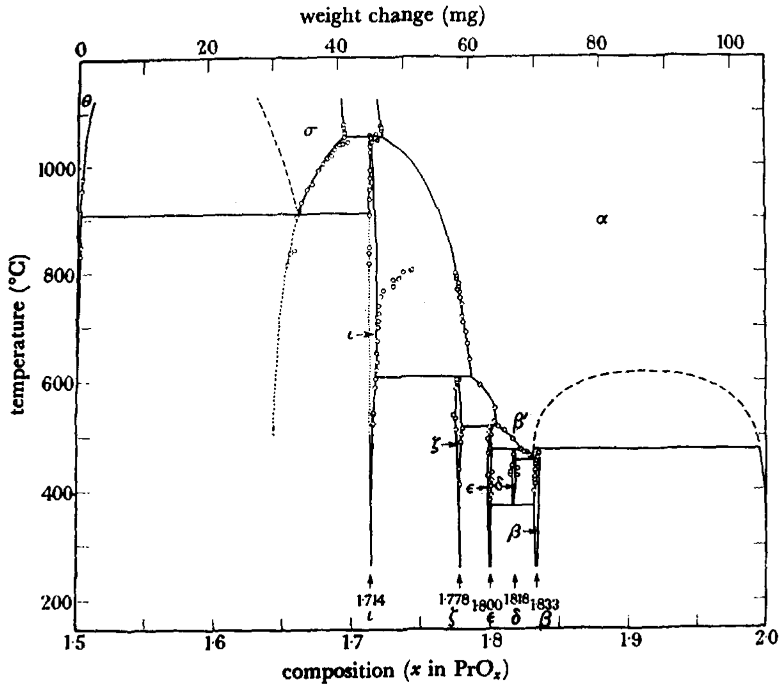

FIG. 1. Phase diagram of the PrO_x–O_2 system.

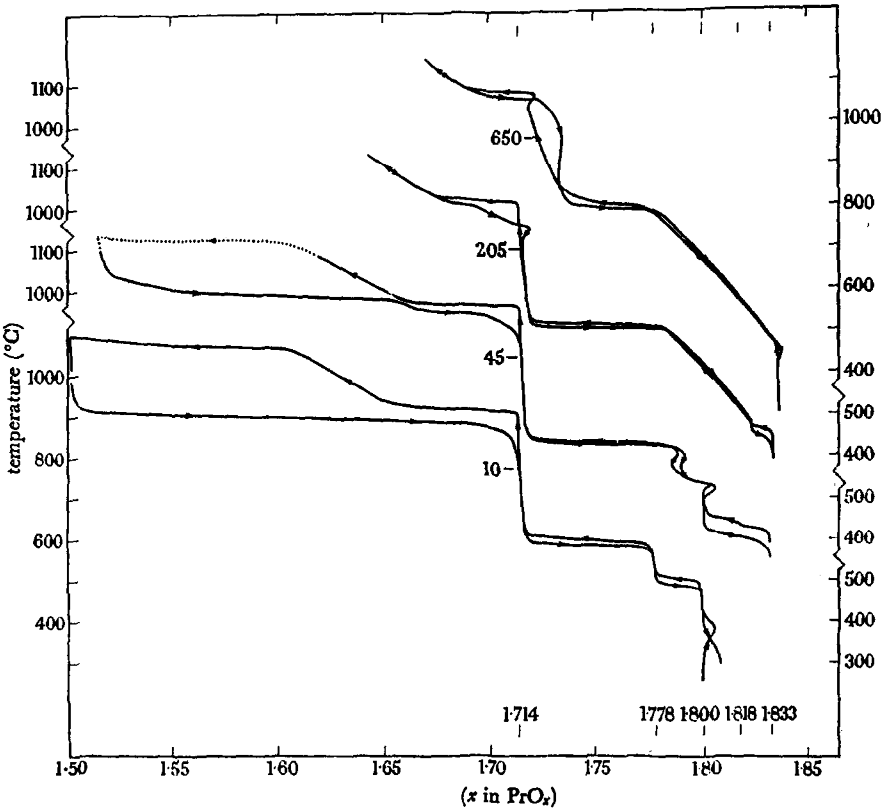

FIG. 2. Selected isobaric cycles in the PrO_x–O_2 system.

the paths of reaction in the two-phase regions between are clearly seen.

Some of the these phases and phase relationships exist in the cerium–oxygen system (*4*) and in the terbium–oxygen system (*5*). All phases both stoichiometric and nonstoichiometric, except for the hexagonal *A*-form sesquioxide polymorphs of cerium and praseodymium and the *B*-form Tb_2O_3, are related to the fluorite structure. The structural principle accounting for these related series of phases has been thought to be strings (of varying length, density, and ordering) of six coordinated metal atoms formed by loss of oxygen from the RO_8 coordination cubes of the fluorite structure (*6*).

In the present discussion attention is focused on the composition region around $MO_{1.714}$. In this region the $Pr_7O_{12+\delta}$ phase is observed to transform to nonstoichiometric phases designated σ in reduction and α in oxidation. In the terbium oxygen system the α phase has not yet been observed and an ordered δ phase is formed in oxidation. Both pure and mixed rare-earth oxide systems shall be described.

Transitions between a Stoichiometric Phase and Contiguous Nonstoichiometric Phases

The Pure PrO_x–O_2 and TbO_x–O_2 Systems.

X-ray diffraction studies indicate that the σ phase is a body-centered-cubic (bcc) structure related to the *C*-type sesquioxide, the ι phase is a rhombohedral structure and the α phase is the face-centered-cubic (fcc) fluorite structure. The close relationships between these structures have previously been pointed out (*5*). The similarity of the X-ray powder diagrams, except for lattice parameter shifts, caused them to be undistinguished for a long time. They were considered simply specimens of a grossly nonstoichiometric fluorite phase. However, diffraction patterns of greater resolution particularly of annealed samples show clearly the transition in reduction from a fcc structure with variable lattice parameter at higher compositions to a rhombohedral phase with virtually no variability in lattice parameters to a bcc phase with variable cell edge at lower composition ranges (*7*).

If one views the fluorite structure as MO_8 coordination cubes in which all edges are shared the variability of composition in the α phase may be due to strings of distorted MO_6 octahedra intergrown in the lattice and distributed along all four $\langle 111 \rangle$ directions increasing in concentration as oxygen is removed. These defects may be clustered in various ways, depending on the pressure, to give structures with short-range order (*8*). In the M_7O_{12} (ι phase) all the strings are along one $\langle 111 \rangle$ direction and each is surrounded by a sheath of MO_7 polyhedra yielding a structure in which the metal atoms are all six or seven coordinated but only slightly shifted from the fluorite positions. The σ phase may have disordered strings in all four $\langle 111 \rangle$ directions as in the α phase but now they are interlocked and are the principal feature of the structure with regions of ι-like domains in between. In the *C*-type sesquioxide the strings of six coordinated metal atoms are of infinite length, nonintersecting, and in all $\langle 111 \rangle$ directions.

In terms of the structural feature (strings?) it is suggested that one goes from long-range disorder → order → disorder as one traverses the region $\alpha \rightleftharpoons \iota \rightleftharpoons \sigma$. Similarly, one may traverse order ⇌ disorder in the $\alpha \rightleftharpoons \epsilon$, $\alpha \rightleftharpoons \delta$ or $\alpha \rightleftharpoons \beta$ reactions or order ⇌ order ⇌ disorder reactions in the $\beta \rightleftharpoons \delta \rightleftharpoons \epsilon \rightleftharpoons \alpha$ reactions (*9*). Short-range order may be strictly held in all phases.

Because of the close similarity of all phases involved, coherent intergrowth [(*1*) and (*10*)] would not be unexpected. This condition must be responsible for the complicated reaction patterns seen in the tensimetric studies of the two-phase regions. Figure 3 illustrates the complex behavior of such transformations in the $\alpha \rightleftharpoons \iota \rightleftharpoons \sigma$ region (*3*). The curves between 60–715 Torr show the path of transit of the system from α on the right (not shown) through ι in the center (steep verticle curves) to σ on the left, and return. The curves have been observed to preserve their general appearance [(*11*) and (*8*)] even when the transit times are increased by orders of magnitude, provided one completes the loop to single phases at both ends.

The curves have been interpreted as follows (*3*). At pressures between 60 and 150 Torr O_2 the behavior is reasonably simple; the α phase decomposes across a two-phase blade to ι, the ι phase suffers a small loss of oxygen as heating is continued until it becomes unstable (at approximately stoichiometric composition) with respect to σ. Decomposition to σ occurs across a two-phase blade at temperatures increasing from about 960–1000°C as the pressure is increased. Upon cooling, the σ phase oxidizes reversibly until it becomes unstable with respect to ι, but instead of transforming rapidly to ι it does so along an almost linear diagonal path, which has been termed a pseudophase ($\sigma\iota$) because of its reproducible bivariant character. When the composition of the pseudophase reaches that of ι as seen in reduction it rejoins the heating curve in reverse, however it does show a narrow hysteresis loop in the

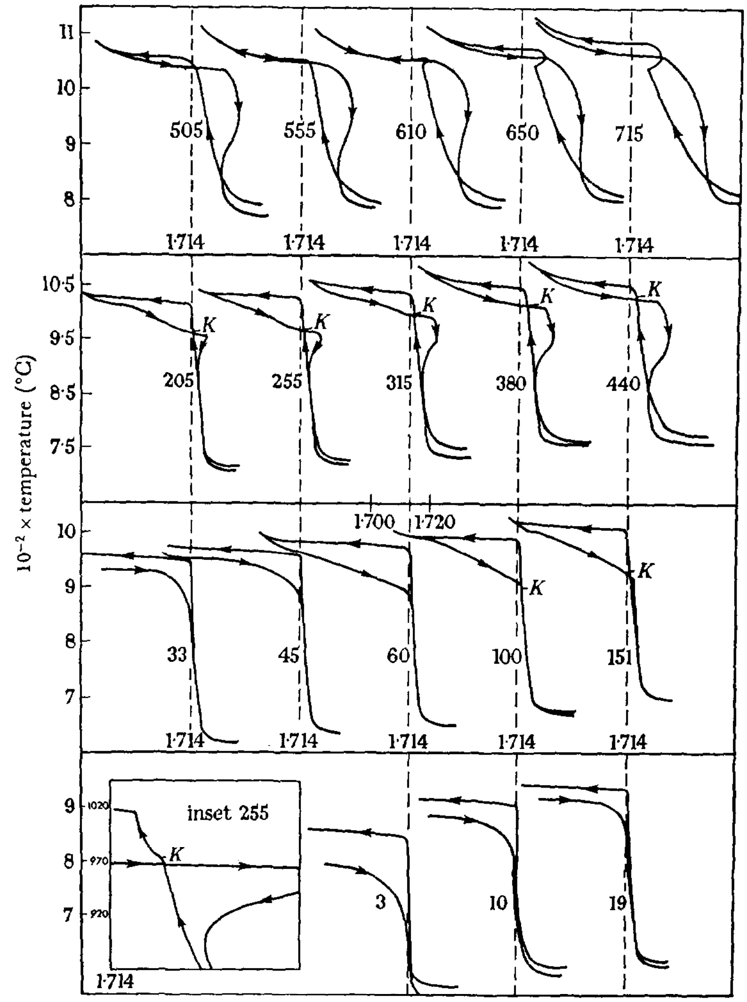

Fig. 3. Isobaric curves in the region $PrO_{1.714\pm\delta}$.

$\iota + \alpha$ region before traversing the α region in coincidence with the heating curve. In short, the sequence is $\alpha \rightarrow \alpha + \iota \rightarrow \iota \rightarrow \iota + \sigma \rightarrow \sigma$ then $\sigma \rightarrow \sigma\iota \rightarrow \iota \rightarrow (\alpha + \iota)' \rightarrow \alpha$. This differs dramatically from classical behavior because of (a) the occurrence of slightly sloping lines in the two-phase regions during heating, due perhaps to "small systems" effects (*12*), (b) the appearance of the anamolous pseudophase behavior in the $\sigma \rightarrow \iota$ region, and (c) the appearance of hysteresis in both of the two-phase regions.

In the pressure range 151 → 555 Torr (see also curve 205 of Fig. 2) there is an evolution of the behavior of the system. This has been explained in terms of the metastable extension of the α and σ regions designated α^m and σ^m. The sequence of events is thought to approach $\alpha \rightarrow \alpha + \iota \rightarrow (\alpha\iota) \rightarrow \iota \rightarrow \iota + \sigma \rightarrow \sigma$ then $\sigma \rightarrow (\iota + \sigma$ or $\sigma^m) \rightarrow (\iota$ or $\alpha^m) \rightarrow (\alpha\iota) \rightarrow (\alpha + \iota)' \rightarrow \alpha$. The symbol $(\alpha\iota)$ is inserted to denote the increasing apparent range of stoichiometry which becomes a dominant feature at higher pressures. The symbol $(\alpha + \iota)'$ designates one branch of a two-phase region showing hysteresis. Metastable α (α^m) is seen to form in oxidation and then decay back to $\alpha\iota$ or ι before returning to α at lower temperatures, accounting for the growing reversal observed. The effects of the existence of α^m is also seen in the kink "K" of the $\alpha\iota$ heating curve.

The new feature in the curves of pressures greater than 555 Torr is the increasing reversal in the $\alpha\iota$ heating curve at high temperature interpreted as $\alpha\iota \rightarrow \alpha$ across a falling two-phase blade followed by $\alpha \rightarrow \sigma$ across the miscibility gap and then cooling in the sequence $\sigma \rightarrow \alpha \rightarrow \alpha\iota \rightarrow (\alpha + \iota)' \rightarrow \alpha$. It might be noticed that the $\alpha + \iota$ region is narrowing and the $\alpha\iota$ approach to ι is more pronounced as the pressure is increased. At the highest pressures, and hence the highest temperature, at any composition, no indication remains of the formation of pure ι or the metastable σ^m or α^m.

This same composition region in the TbO_x–O_2 system resembles PrO_x–O_2 at the lowest pressures (*11*), as seen in Fig. 4. The sequence of phase reactions is seen to be δ (ordered $TbO_{1.818}$) $\rightarrow \delta + \iota \rightarrow \iota \rightarrow \iota + \sigma \rightarrow \sigma$ then $\sigma \rightarrow \sigma\iota \rightarrow \iota \rightarrow (\delta + \iota)' \rightarrow \iota\delta \rightarrow \delta$. Since the α phase does not appear in any TbO_x–O_2 isobar up to the highest pressures studied, we shall confine our attention in this case to the $\iota \rightleftharpoons \sigma$ transformation. The interpretation of this region is the same as for praseodymium oxides in the 60 → 150 Torr range, with the pseudophase $\sigma\iota$ the most interesting feature. The inaccessibility of the α or α^m fields simplifies the system very much. Isobar 200.6 was repeated with ample time given for equilibrium to be reached at each point and no change was observed in the $\iota \rightarrow \sigma$ region. However, a significant reduction in the hysteresis loop in the $\delta \rightarrow \iota$ region was observed (as indicated by the dotted line) but with no change in the $\iota\delta$ pseudophase.

The appearance of pseudophase behavior is most striking in cases where there is a loss of symmetry as in $\sigma \rightarrow \iota$, $\alpha \rightarrow \iota$, $\iota \rightarrow \delta$. It is clear, however, that the reverse types of reactions (with gain in symmetry $\delta \rightarrow \iota$, $\iota \rightarrow \sigma$, $\iota \rightarrow \alpha$) also show some slope in the $(x, T)_P$ curves but of a much smaller magnitude.

The same region seen from the point of view of isothermal runs on very pure samples of PrO_x and TbO_x confirms the gross features seen in the isobars (*11*).

From the discussion so far, it should be apparent that a generalized set of phase reactions are proposed which provide an "understanding" of the tensimetric data in the PrO_x–O_2 and TbO_x–O_2 systems in the regions contiguous with the M_7O_{12} phase. Suppose we see how these same transformations are revealed by diffracted X-rays in isobaric runs (*13*) in PrO_x.

A sample of PrO_x was exposed, at temperature intervals, to X-rays while the oxygen pressure was held constant. The temperature was increased in steps to about 1100°C and returned to room temperature in each cyclic isobaric run. The diffraction patterns were indexed and the calculated lattice parameters plotted against temperature for 100, 320, and 700 Torr isobars.

This study confirmed the above interpretation in all the single-phase and two-phase regions in that the expected X-ray patterns were seen. Even though, for example, the $\iota + \sigma$ and $\iota + \alpha$ isobars do have a significant slope, they were followed carefully at 320 and 700 Torr, respectively, at frequent temperature intervals and were seen to be diphasic all the way with appropriate quantities of each phase in both cases. In the cooling cycle of the 320-Torr isobar it was not possible to confirm the $\sigma^m \rightarrow \alpha^m$ transition; only the ι phase of normal lattice parameter was observed as the product.

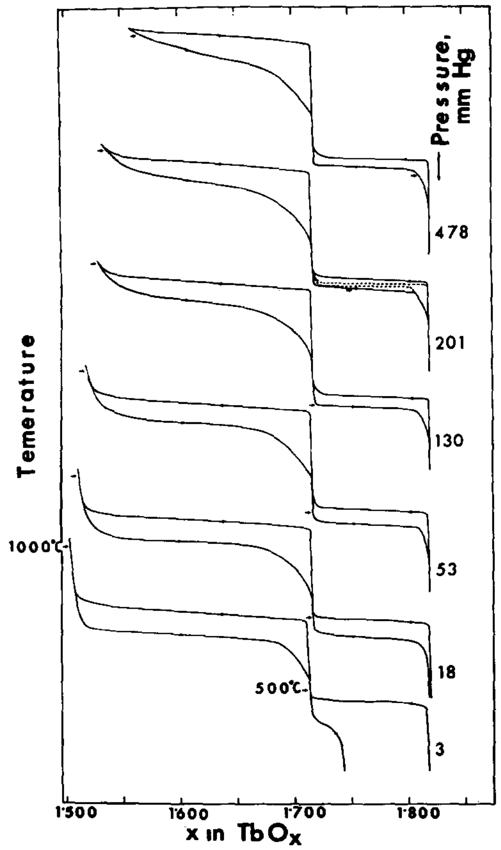

FIG. 4. Isobaric cycles in the TbO_x–O_2 system.

The diffraction patterns in the 700-Torr isobar in the $\alpha \rightarrow \alpha\iota \rightarrow \iota$ region always showed two phases, α and ι, with ι growing at the expense of α over the temperature range of 863 → 992°C. In oxidation in this temperature region the ι phase was observed to decrease as the α phase increased. At 769°C the environmental conditions were maintained overnight with no change occurring in the relative intensities of the diffraction lines indicating the great stability of this pseudophase.

Subsequent high-temperature diffraction work (*9*) with specific purpose to examine this pseudophase behavior in the $\alpha\iota$ region in greater detail showed it to appear diphasic to the X-rays over its entire existence range.

Similar high-temperature X-ray diffraction studies of the TbO_x–O_2 system were made (*14*), with the result that only δ, ι, and σ phases were observed and all two-phase regions or pseudophase regions appeared diphasic to the X-rays. There was agreement between isobaric and isothermal runs in this respect.

In summary, the X-ray diffraction studies suggest single phases in all the expected single-phase regions and two phases in nearly all the hysteresis loops, including the pseudophase regions. This corroborates the main features of the interpretation of the tensimetric measurements but presents certain problems with respect to the nature of the pseudophase regions. This paradox will be discussed below.

The Mixed Praseodymia–Terbia–Oxygen System

Isobaric studies have been made (*11*) on the ternary system Pr–Tb–O_2 in the oxygen pressure range of 0–1 atm and temperature span of 0–1100°C. Compositions at 25 atom% intervals were investigated. The results of the 320-mm isobars for the pure end-members and the mixtures are shown in Fig. 5. Only the $Pr_{0.25}$–$Tb_{0.75}O_x$ isobar could be considered as in any way intermediate to the behavior of the two pure phases.

Couched in the language of the preceding sections one observes the relative increase in the stability of the nonstoichiometric phases, α and σ, and the relative decrease in the stability of any ordered intermediate phases. In fact only the ι phase is strongly inferred.

As between PrO_x and TbO_x the ι phase is much more stable in the latter at the same temperature and pressure. This is paralleled with the intrusion of the α phase in the PrO_x system at higher temperatures, which at the highest pressures generates the $\alpha\iota$ pseudophase.

With the addition of 25 atom% terbium the ι phase is not seen; rather the α and σ phases together with the miscibility gap between them fill the entire region. In many ways these isobars are what might be expected at much higher pressures for the pure PrO_x system. In the 50:50 mixture the behavior is similar except for a faint break at about $RO_{1.8}$ in the α region.

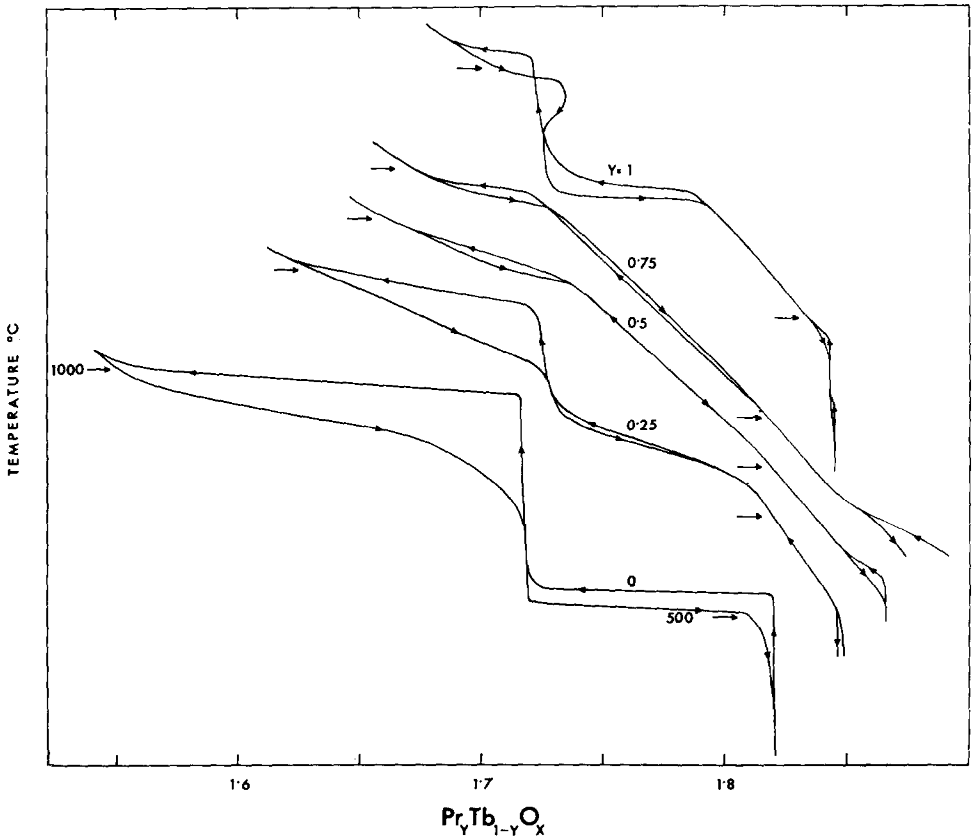

FIG. 5. Representative isobars in the $Pr_yTb_{1-y}O_x$–O_2 system.

For 75 atom% terbium the break at about $RO_{1.8}$ has become a prominent feature of the curves, indicating an anticipatory wrinkle in the α free-energy surface in the region of the ordered phases in the pure systems. More obvious, however, is the appearance of the ι phase and the generation of the contiguous hysteresis loops and the $\sigma\iota$ pseudophase characteristic of the pure phases. Indeed, these curves resemble the higher pressure PrO_x curves without the complication of the σ^m and the α^m metastable phases.

The behavior of the mixed oxides suggests the following. The formation of the ordered phases involves the ordering of a large cluster of atoms. The phase is stable when this cluster has favorable low free-energy. Focusing on the ι phase which is most stable in TbO_x these results indicate that clustering is possible until more than one-fourth of the Tb atoms have been replaced at random by Pr, but beyond that the disordered phases are more stable under any conditions reached in the experiments. Looked at from the other side, the ι phase in PrO_x is stable, but even low concentrations of foreign atoms disturbs the system such as to destroy the clusters in favor of the α and σ phases with the miscibility gap, except perhaps at the very lowest pressures.

The X-ray diffraction results of Brauer (*15*) on this system of mixed oxides indicated the existence of a rhombohedral phase at concentrations as great as 15 atom% praseodymium in terbium oxide when the sample was quenched, and a cubic (α) phase when the sample was cooled slowly, even though this latter phase is not present in the pure terbium oxide system.

The Terbia–Ceria–Oxygen System

Extensive tensimetric studies, both isobaric and isothermal, have been carried out on the $Ce_yTb_{1-y}O_x$ system (*16*). Only a few comments on the ι region will be made here.

Figure 6 illustrates the results obtained from terbia containing 20 mole% ceria. At low pressures, a broadened ι phase is seen and the phase transitions could be stated as $\alpha \rightarrow \alpha + \iota \rightarrow \iota$ (or $\alpha\iota$) $\rightarrow \sigma$ then $\sigma \rightarrow \sigma\iota \rightarrow \iota$ $(\iota\alpha) \rightarrow (\alpha + \iota)' \rightarrow \alpha$. At highest pressures the ι phase does not decompose.

These results are similar to those with 75:25 atom% terbia–praseodymia previously discussed, except for the relatively greater oxygen pressure above terbia–praseodymia mixtures. To a first approximation (a conclusion reached in the broader study (*16*)], there appeared to be no valence stabilization of the cerium. However, the appearance of the α phase indicates a definite interaction, since it would not be seen to this extent in ceria under these conditions nor seen at all in the terbia system.

An isothermal study of the $Ce_yTb_{1-y}O_x$ system in the pressure range 10^{-6} to 1 atm confirmed the general features seen in the isobaric studies.

High-temperature X-ray diffraction was observed for isobaric runs on the $Ce_{0.2}Tb_{0.8}O_x$ system (*14*). In general, the quality of the diffractometer traces was poor. The low-angle peaks were reasonably sharp but the K_α doublets were unresolved at high angles. Annealing did not appreciably improve the patterns. Although no indication of loss of symmetry was confirmed in the patterns there is a striking variation in the lattice parameter to suggest the phase sequence $\delta \rightarrow \alpha \rightarrow \alpha + \iota \rightarrow \iota \rightarrow \sigma$. Of course, the limits of error of the measurements were greater than in the pure systems, and it is apparent that the compositional range of the ι phase is greater as indicated in the isobars (Fig. 6). The diffraction peaks are broadened in the ι region but not resolved, probably indicating rhombohedral distortion. The peaks narrowed again in the σ region but the superstructure lines were not seen.

Thermodynamical Considerations

Even a glance at the isobaric and isothermal curves in the region adjacent to the ι phase in these systems is enough to convince one that they are nonequilibrium in the classical sense. So much so, in fact, that one might dismiss any serious consideration of the thermodynamic properties of a system undergoing these unorthodox transitions. In spite of this, certain observations indicate that these are exceptionally durable nonequilibrium situations. For example, it was observed at an early time that so long as one began with a single phase and went through the sequence of transitions showing hysteresis phenomena to another single-phase region before the path was reversed, the completed loops were nearly identical in shape and position. Remember that the 201-mm isobar of the TbO_x (Fig. 4) system was circumtraversed with each point taken at equilibrium. The equilibrium curve was essentially super-imposable on the 1.3°C/min curve to the left of ι. The loop to the right of ι was appreciably reduced in area but all the significant features were preserved undiminished, including the $\iota\delta$ pseudophase.

A corresponding "equilibrium" trace of the 320-mm isobar of the PrO_x–O_2 system, was essentially identical with the 1.3°C/mm run, except for a decrease in the $(\alpha + \iota)$ loop. All the essential

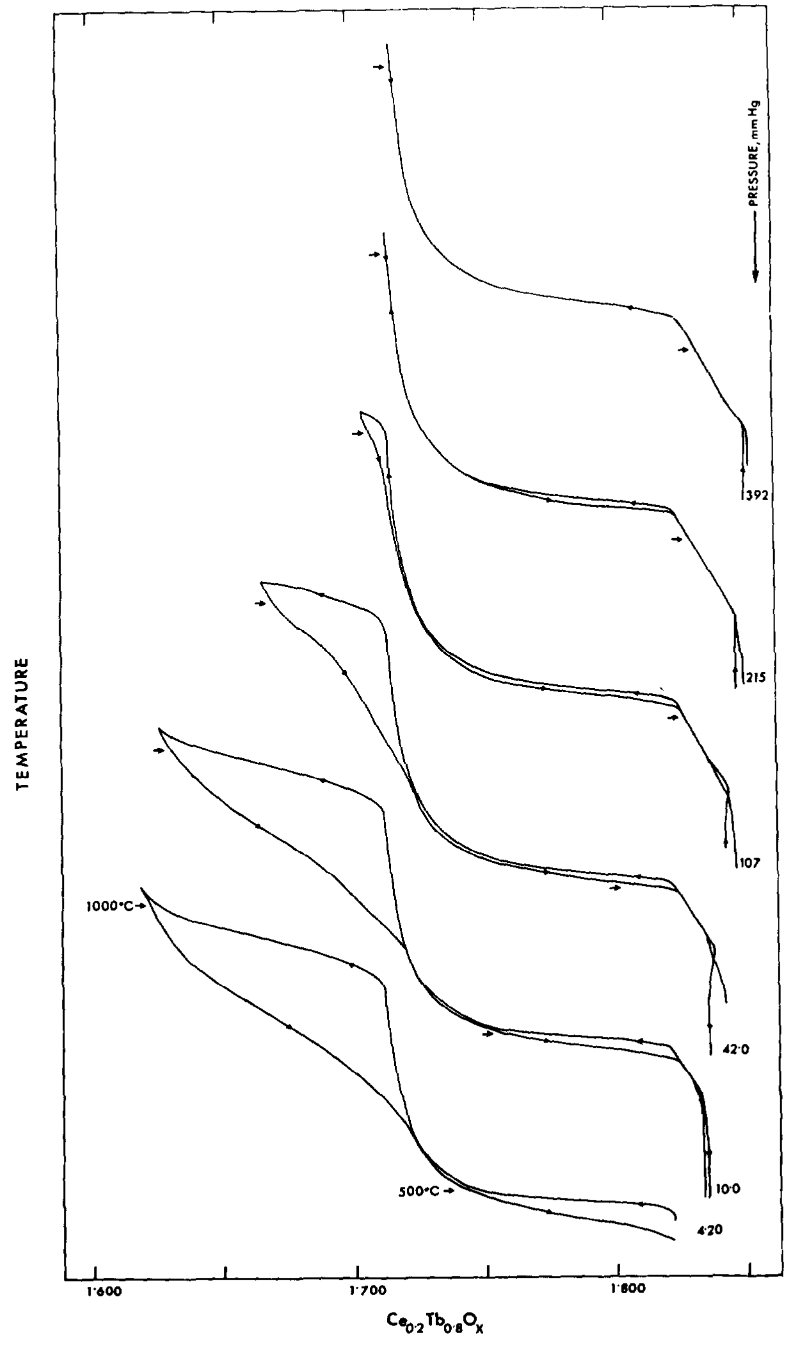

FIG. 6. Isobars in the $Ce_{0.2}Tb_{0.8}O_x$–O_2 system.

features of the transitions were preserved exactly, including $\alpha\iota$, $\sigma^m \rightarrow \alpha^m$, and the $\alpha^m \rightarrow \alpha\iota$ reversal.

The phase diagram of PrO_x (Fig. 1) was constructed by picking off the temperature and composition of each indicated phase transition from each isobar. These data, plotted as $RT\ln p$ against T, are only slightly different in heating and cooling (*3*). All the transitions observed are well behaved in this kind of treatment, even including the metastable changes. A similar treatment is possible for the TbO_x–O_2 data (*5*) and for the mixed praseodymia and terbia.

In view of this reproducibility, it was of interest to treat the hysteresis loops to the left of ι phase in the TbO_x–O_2 system as equilibrium phenomena. Accordingly, the partial molar free energy of solution of oxygen in the oxide ($-RT\ln P_{O_2}$) was calculated for each branch of the loop *(11)* and the derived partial molar enthalpy and entropy values calculated. The entropy values in the $\iota \rightarrow \alpha$ transition for the reduction curve are classically constant until the σ phase is approached, at which point they become more positive rapidly and should be relatively small for oxygen going into random positions in the σ phase near the $TbO_{1.5}$ composition.

The oxidation branch of the curve which represents transit via the $\sigma\iota$ pseudophase is more interesting. It shows a rapid increase in entropy change as oxygen is added and instead of leveling off, as would be characteristic of a two-phase region, it continues to rise until it peaks above the value for the reduction curve at a composition of $TbO_{1.69}$. The greater entropy changes (at a point) in oxidation near the maximum suggest greater order of the pseudophase than for the two-phase system at the same composition. A more surprising result is the maximum in the entropy curve at $TbO_{1.69}$ just as the $\sigma\iota$ pseudophase is established. The curves do not close, as they must if the cycle were complete, hence there must be changes beyond the extremities to bring this about, or, more likely, the two σ and ι phases are not exactly equivalent.

This description of the phase reactions in the vicinity of a stable intermediate compound of slightly variable composition, and how they are influenced by admixture of similar atoms, points up the extremely complex behavior of solid materials. Such complexities revealed by tensimetric measurements and confirmed in part by X-ray powder diffraction at temperature suggest profound and intricate structural changes of the level David Wadsley has reported for natural intergrowth systems *(17)* and for the many intergrowth block structures described in many of his later publications. The structural elements responsible for the rich variability observed in the rare-earth oxide systems is not crystallographic shear and has not been adequately described, but may involve three-dimensional blocks because of the greater isotropy of this cubic related system.

Acknowledgment

It is a pleasure to express appreciation to the Atomic Energy Commission for support of the entire program from which this thin slice is taken.

References

1. See J. S. Anderson, *in* "Recent Progress in the Investigation of Nonstoichiometry" (A. Rabenau, Ed.), North-Holland Publ. Co., in press; and J. S. Anderson, *in* "Chemistry of Extended Defects in Non-Metallic Solids" (L. Eyring and M. O'Keeffe, Eds.), North-Holland Publ. Co., in press, for detailed reviews of thermodynamic considerations and references to the literature.

2. A. R. Ubbelohde, *J. Chim. Phys.* 33 (1966); "Melting and Crystal Structure," Oxford Univ. Press, London, England 1965.

3. B. G. Hyde, D. J. M. Bevan, and L. Eyring, *Phil. Trans. Roy. Soc. London Ser. A.* **259**, 583 (1966).

4. D. J. M. Bevan and J. Kordis, *J. Inorg. Nucl. Chem.* **26**, 1509 (1964).

5. B. G. Hyde and L. Eyring, *in* "Rare Earth Research III" (L. Eyring, Ed.), p. 623, Gordon and Breach, New York, 1966.

6. B. G. Hyde, D. J. M. Bevan, and L. Eyring "International Conference on Electron Diffraction and Crystal Defects," Melbourne II C-4, (1965), Published and distributed for the Australian Academy of Science by Pergamon Press, 1966.

7. J. O. Sawyer, B. G. Hyde, and L. Eyring, *Bull. Soc. Chim. France* 1190 (1965).

8. M. S. Jenkins, R. P. Turcotte, and L. Eyring, *in* "Chemistry of Extended Defects in Non-Metallic Solids," (L. Eyring and M. O'Keeffe, Eds.), Chap. 3, North Holland Publ. Co., in press.

9. R. P. Turcotte, M. S. Jenkins, and L. Eyring, unpublished work, See AEC report C00-1109-46.

10. Sten Andersson, W. G. Mumme, and A. D. Wadsley, *Acta Cryst.* **21**, 802 (1966).

11. J. Kordis and L. Eyring, *J. Phys. Chem.* **72**, 2044 (1968).

12. T. L. Hill, "Thermodynamics of Small Systems," Part 1, Chap. 5, W. A. Benjamin, Inc., New York, 1963.

13. D. Arthur Burnham and LeRoy Eyring, *J. Phys. Chem.* **72**, 4415 (1968).

14. D. Arthur Burnham, LeRoy Eyring, and J. Kordis, *J. Phys. Chem.* **72**, 4424 (1968).

15. G. Brauer and B. Pfeiffer, *in* "Rare Earth Research III" (L. Eyring, Ed.), p. 573, Gordon and Breach, New York, 1965. Also *Z. Anorg. Allgem. Chem.* **341**, 238 (1965).

16. J. Kordis and L. Eyring, *J. Phys. Chem.* **72**, 2030 (1968).

17. A. D. Wadsley, *in* "Nonstoichiometric Compounds" (L. Mandelcorn, Ed.), p. 98, Academic Press, Inc., New York, 1964.